horticulturae

MDPI

Article

Potential Metabolic Pathways and Related Processes Involved in Pericarp Browning for Postharvest Pomegranate Fruits

Xiaoxiao Qi [1,2,†], Jianrong Zhao [1,3,†], Zhenyu Jia [4], Zhen Cao [1,5], Chunyan Liu [1,5], Jiyu Li [1,5], Ying Su [1,5], Yongbao Pan [6], Cong He [1,5], Yiliu Xu [1,*] and Gaihua Qin [1,5,*]

1 Key Laboratory of Germplasm Innovation and Utilization of Horticultural Crop, Ministry of Agriculture and Rural Affairs, Anhui Key Laboratory of Genetic Improvement and Ecophysiology of Horticultural Crop, Institute of Horticultural Research, Anhui Academy of Agricultural Sciences, Hefei 230031, China
2 College of Agriculture, Medicine and Health, Anhui Open University, Hefei 230022, China
3 College of Resource and Environment, Anhui Science and Technology University, Fengyang 233100, China
4 Department of Botany and Plant Sciences, University of California, Riverside, CA 92521, USA
5 Key Laboratory of Fruit Quality and Development Biology, Anhui Academy of Agricultural Sciences, Hefei 230001, China
6 Sugarcane Research Unit, Agricultural Research Service (USDA), United States, Houma, LA 70360, USA
* Correspondence: yiliuxu@163.com (Y.X.); qghahstu@163.com (G.Q.)
† These authors contributed equally to this work.

Abstract: Pericarp browning occurs widely in postharvest pomegranate fruit, but little is known about its mechanism. In this study, 'Baiyushizi', a browning-sensitive cultivar, was used to investigate the physiological and genetic changes during pericarp browning. The pericarp browning index (BI) increased greatly after 3 d storage at room temperature, and, consequently, the fruit appearance became unattractive after 6 d. The increasing concentration of malondialdehyde (MDA) and electrolyte leakage were detected in browning pericarp. Polyphenol oxidase (PPO) activity increased significantly after 3 d, while ascorbate peroxidase (APX) and catalase (CAT) activity decreased steadily during storage. Total phenolics content decreased gradually during storage, while ascorbic acid (AsA) and glutathione (GSH) contents increased firstly, then declined. Differentially expressed genes (DEGs) of pericarp under different browning degrees were identified in the metabolic processes of phenolic compounds, lipids, ascorbic acid, glutathione, sugar, starch, energy-related, ethylene biosynthesis and signal transduction pathways. Accordingly, the potential metabolic pathways and related processes involved in pericarp browning were described. The results not only provided insights on the genetic mechanism of pericarp browning in pomegranate but also guidance on controlling postharvest fruit browning in general.

Keywords: pericarp browning; pomegranate; physiological change; candidate genes

Citation: Qi, X.; Zhao, J.; Jia, Z.; Cao, Z.; Liu, C.; Li, J.; Su, Y.; Pan, Y.; He, C.; Xu, Y.; et al. Potential Metabolic Pathways and Related Processes Involved in Pericarp Browning for Postharvest Pomegranate Fruits. *Horticulturae* **2022**, *8*, 924. https://doi.org/10.3390/horticulturae8100924

Academic Editor: Isabel Lara

Received: 12 September 2022
Accepted: 5 October 2022
Published: 8 October 2022

1. Introduction

Pomegranate (*Punica granatum*) is a perennial fruit tree, widely cultivated in countries with Mediterranean-like climates around the world, including Tunisia, Turkey, Spain, Egypt, Morocco, the USA, China, India, Argentina, Israel, and South Africa [1,2]. Pomegranate fruit is widely consumed due to distinguished nutritional and medicinal values. The fruit is referred to as superfruit 'Baiyushizi', which is also called Sanbai pomegranate (*Bai* is white in China) for its white flowers, seeds, and pericarp. 'Baiyushizi' is a widely planted cultivar in Anhui Province, China. The white fruit is unique and desirable to most consumers, leading to increasing popularity in China. However, 'Baiyushizi' is a browning-sensitive cultivar and the browning of white pericarp has severely affected its fruit quality and marketability. Thus, it warrants a study on the mechanism of pericarp browning for the maintenance of the harvested pomegranate fruit.

Fruit browning may involve enzymatic or/and non-enzymatic processes [3]. A variety of non-enzymatic reactions, including the Maillard reaction, vitamin C oxidation,

caramelization, and the chemical oxidation of phenolics, may contribute to pericarp browning [4,5]. Non-enzymatic endogenous antioxidant substances, such as glutathione (GSH) and ascorbic acid (AsA) [6], increase the capacity of scavenging reactive oxygen species (ROS), alleviate membrane lipid peroxidation, maintain the integrity of cellular membrane structure, and accordingly, inhibit pericarp browning [7]. Furthermore, the imbalance in ROS metabolism due to an excessive accumulation of malondialdehyde (MDA), quickly causes oxidative damage of the cellular membrane and affects the storage quality and pericarp browning [8] (Lin et al. 2014). Enzymatic reaction processes, polyphenol oxidase (EC 1.10.3.1, PPO), phenylalanine ammonia lyase (EC 4.3.1.24, PAL), peroxidase (EC 1.11.1.7, POD), catalase (EC 1.11.1.6, CAT), and superoxide dismutase (EC1.15.1.1, SOD) may cause the most devastating browning [9–14]. Especially, a few active oxygen-scavenging enzymes, such as SOD, CAT and APX, may be responsible for the development of browning [15]. Previous studies showed that the expression of genes encoding these enzymes were changed during the browning of fresh-cut fruit and vegetables [16]. It has also been reported that the expression of genes involved in carbohydrate and hormone metabolism also changed during the browning of pears and sponge gourd fruit [17,18]. Studies were also conducted to measure the phenolics content, antioxidant capacity, and related enzyme activities in the browning pericarp of pomegranate fruit [19,20]. Qi and Qin reported changes in reducing sugar and amino acid nitrogen contents, 5-hydroxymethylfurfural, PPO activity, and free radical scavenging ability in pomegranate pericarp during storage [21]. To obtain a global view of browning mechanisms during fruit storage, the physiological and genetic changes in the pericarp of 'Baiyushizi' fruit stored at room temperature were investigated. The results may provide a guide for the development of a management plan to control fruit browning.

2. Materials and Methods

2.1. Plant Materials

'Baiyushizi' fruit were harvested at commercial maturity (<0.50% of titratable acidity; >15.0% of total soluble solid) from a commercial orchard in Huaiyuan County, Anhui Province. The fruit were transported on the same day to the Key Laboratory of Genetic Improvement and Ecophysiology of Horticultural Crop (Hefei) in a foam box in approximately 4 h. Fruit of uniform size without any visible damage were selected for storage at room temperature (25 ± 2 °C) for 0~6 d. To survey the browning index (BI) and physiological changes for fruits during pericarp browning, three replications were set up. Each replication involved seven groups with six fruit per group. Disc pieces of exocarp (outer pericarp), about 10 mm diameter and 2 mm thickness, were used for assaying electrolyte leakage. Ten grams of exocarp tissues were dissected from fruit hip (Figure S1) and were immediately frozen in liquid nitrogen and stored at −80 °C for further study. Physiological parameters related to browning were detected for fruits during the storage period. Pericarps of fruit stored for 0, 3 and 6 d, noted as 0 d (control), 3 d (RTS3) and 6 d (RTS6), respectively, were selected to survey the transcriptome profiles.

2.2. Evaluation of Browning Index

The browning index (BI) of the pericarp was evaluated according to the method of Zhang and Zhang with a little modification [19]. The browning level and appearance scale (score) were judged according to the visual appearance of the pericarp: 0 (0 score), no browning and glabrous surface, excellent quality; 1 (25 score), a slight browning, tarnished and smooth surface; 2 (50 score), a slight browning and loss of water; 3 (75 score), obvious browning and severe loss of water; and 4 (100 score), serious browning and pericarp crumpled, pool quality. Finally, the BI was calculated using the following equation: BI = $\sum$ (browning scale × proportion of corresponding fruit within each class).

2.3. Malondialdehyde Concentration Measurement

Malondialdehyde (MDA) was measured according to the procedure of Sun et al. [22]. One gram of pericarp samples was homogenized in 4 mL of 0.5% trichloroacetic acid (TCA) and centrifuged at 10,000× *g* for 20 min. Then, 2 mL of the extract was collected and reacted with 2 mL of 0.67 % thiobarbituric acid (TBA). The mixture was then heated at 100 °C for 20 min and then cooled immediately in an ice-bath for 5 min. The supernatant was centrifuged at 5000× *g* for 10 min to clarify the solution. The absorbance at 450 nm, 532 nm and 600 nm was measured using a spectrophotometer (TU-1810 DSPC, Beijing Puxi Instrument Co., Beijing, China). The MDA concentration was calculated according to the following equation: MDA concentration = $6.45 \times (A_{532} - A_{600}) - 0.56 \times A_{450}$.

2.4. Electrolyte Leakage Determination

The determination of electrolyte leakage was conducted according to Zhu et al. [23]. Twenty disc pieces (10 mm diameter, 2 mm thick) of the pericarp were immersed into 40 mL double-distilled water, and the initial electrolyte leakage was measured as P0 by using a conductivity meter (DDS-307, Shanghai Precise Science Instrument Co., Shanghai, China). After incubating for 10 min, the electrolyte leakage was measured as P1. Then the water was boiled for 10 min, cooled to room temperature, and the electrolyte leakage P2 was measured. Ultimately, the electrolyte leakage was calculated using the following equation: electrolyte leakage (%) = (P1 − P0)/(P2 − P0).

2.5. Determination of Superoxide Dismutase, Catalase, Ascorbate Peroxidase and Polyphenol Oxidase

Superoxide dismutase (SOD), catalase (CAT) and ascorbate peroxidase (APX) were assayed with the methods of Cao et al. [24] and Zhang et al. [25]. One gram of pericarp was homogenized with 10.0 mL of 0.1 M ice-cold phosphate buffer (pH 7.5) containing 1 mM EDTA and 5.0% (m/v) PVP. After centrifugation at 12,000× *g* for 20 min at 4 °C, the supernatant was used to assay the activities of SOD, CAT and APX. The SOD activity assay was performed by using the nitro-blue tetrazolium (NBT) method. One unit of SOD activity was defined as the amount of the enzyme that caused 50% inhibition of NBT reduction at 560 nm. One unit of CAT and APX activity was defined as a change of 0.01 in the absorbance of the reaction solution at 240 nm and 290 nm per minute. The activities of SOD, CAT and APX were represented as U mg^{-1} protein.

Polyphenol oxidase (PPO) activity was measured by employing the method of Wojdyło et al. [26]. One gram of pericarp was homogenized in 3 mL of 50 mmol L^{-1} phosphate buffer (pH 5.5) for 2 h in the dark. The homogenates were centrifuged at 18,000× *g* for 10 min at 4 °C, and the supernatant was collected for PPO activity assay. The PPO activity was expressed as U mg^{-1} protein. One unit (U) was equal to an enzyme quantity that caused an absorbance change of 0.001 units per min.

Protein content was estimated according to Bradford's methodology [27] using bovine serum albumin (BSA) as the standard.

2.6. Ascorbic Acid and Glutathione and Total Phenolics Contents

The content of ascorbic acid (AsA) was assayed following the method of Cai et al. [28]. One gram of pericarp was homogenized in 10 mL of 5 % (*w*/*v*) TCA and then centrifuged at 12,000× *g* for 15 min at 4 °C. The supernatant was collected for the determination of AsA content ($g \cdot kg^{-1}$).

To determine the content of glutathione (GSH), one gram of the pericarp was homogenized in 10 mL of 50 mM sodium phosphate buffer (pH 7.0) and then centrifuged at 12,000× *g* for 20 min at 4 °C. The supernatant was collected and used to assay colorimetrically for GSH content, as described by Li et al. [29] with modification. The reaction mixture contained 0.1M phosphate buffer pH 7.0 (0.5 mL), 4 mM DTNB (0.5 mL, DTNB in 0.1 M phosphate buffer pH 7.0) and crude extract (1 mL). The reaction was run at 25 °C for 10 min. The absorbance at 412 nm was measured; 0.1 M phosphate buffer pH 7.0 (0.5 mL), replacing DTNB, was used as the blank. The GSH content was expressed as $g \cdot kg^{-1}$. The

total phenolics content of pericarp tissue was measured with the Folin–Ciocalteu system. The procedure consisted of a 10 percent combination of 0.5 mL of test solution with 2.5 mL Folin–Ciocalteu reagent. After 5 min, the sample was raised to 1 mL Na_2CO_3 by 20 % (*w*/*v*). The mixture was then shaken vigorously and incubated in the dark for 60 min. The absorbance was eventually calculated at 765 nm [30]. A standard curve of gallic acid was plotted, and the total phenolics content was expressed as $g \cdot kg^{-1}$.

2.7. RNA Extraction, Library Preparation and RNA-Seq

Total RNA was prepared from pericarp samples using the Tiangen RNAprep Pure Plant Kit (Tiangen, Beijing, China) according to the manufacturer's instructions. An Agilent 2100 Bioanalyzer (Agilent RNA 6000 Nano Kit, Palo Alto, CA, USA) was used to determine RNA concentration, RIN value, 28S/18S, and the fragment length distribution. NanoDrop™ (Thermo Scientific, Wilmington, NC, USA) was used to determine the purity of the RNA samples. For cDNA synthesis, equal quantities of high-quality RNA from control, RTS3 and RTS6 samples were pooled. The concentration and quality of each RNA sample was evaluated using an Agilent 2100 Bioanalyzer (Agilent Technologies, Palo Alto, CA, USA). The mRNAs were isolated from total RNA by the oligo (dT) method [31], followed by fragmentation under certain conditions. First and second strands of cDNA were synthesized. cDNA fragments were purified and re-dissolved in EB buffer for end reparation and single nucleotide A (adenine) addition. After that, the cDNA fragments were linked with adapters. cDNA fragments of suitable size were selected for PCR amplification. Three replicates of each sample were sequenced using the Illumina HiSeq Platform by the Beijing Genomics Institute (BGI). After filtering, the clean reads were mapped to reference genome using hierarchical indexing for the spliced alignment of transcripts [32].

2.8. Data Analysis, Annotation and Differential Expression Analysis

The raw reads of nine libraries were subjected to quality trimming and filtering. Adapter was removed by SOAPnuke Software (v1.5.2, https://github.com/BGI-flexlab/SOAPnuke, Accessed on 19 January 2018). Clean reads were mapped to a reference genome using the alignment protocol of Bowtie2 Software [33]. Gene expression levels were calculated using the RSEM software package (v1.2.12, http://deweylab.biostat.wisc.edu/RSEM, Accessed on 23 January 2018) [34] and were expressed using fragments per kilobase per million mapped reads (FPKM). Gene expression analysis was performed using DEGseq, a Poisson-based method described by Wang et al. [35]. DEGseq parameters were set as follows: fold change ≥ 2 and adjusted *P*-value ≤ 0.001. Based on the results from the Kyoto Encyclopedia of Gene and Genomes (KEGG) annotation (https://www.genome.jp/kegg/, Accessed on 23 January 2018), we performed pathway functional enrichment for the differentially expressed genes (DEGs) implemented by phyper.

2.9. Quantitative Real-Time PCR (qRT-PCR)

Six candidate genes, namely, *Pgr016899*, *Pgr025556*, *Pgr020281*, *Pgr013991*, *Pgr013780* and *Pgr009313*, were selected for qRT-PCR validation. Total RNA was extracted from pericarp tissues of 0 d, 3 d and 6 d with TRIzol reagents (Invitrogen, Waltham, MA, USA). First-strand cDNA was synthesized using the PrimeScript™ RT Reagent Kit (TaKaRa, China) following the manufacturer's instructions. Primers were designed using Primer Premier 5.0 (http://www.premierbiosoft.com, Accessed on 16 February 2018), and primer sequences are shown in Table S1. The qRT-PCR was conducted using the TB Green® Premix Ex Taq™ (TaKaRa, Beijing, China) on an ABI StepOne Plus thermocycler (Applied Biosystems, Foster, CA, USA). The relative quantification of candidate genes was performed using the cycle threshold (Ct) $2(^{-\Delta\Delta Ct})$ method with *Pgractin7* as an internal control. Relative expression levels of candidate genes were illustrated using GraphPad Prism 6.01 (GraphPad Software Inc., La Jolla, CA, USA). The expression levels of the genes obtained in RNA-seq and qPCR were compared with the Pearson correlation coeffcient.

2.10. Statistical Analyses

Data was expressed as means ± standard deviation (n = 3) and analyzed by one-way analysis of variance (ANOVA) with least significant differences at the 0.05 level using SPSS 17.0 Statistics (SPSS Inc., Chicago, IL, USA).

3. Results

3.1. Appearance and BI Changes of Pericarp of Postharvest Fruit

The pericarp of fresh fruit from the 'Baiyushizi' variety was white and bright. The pericarp became light yellow when the fruit was harvested and stored at room temperature for the original 2 d. Then pericarp browning was visible (Figure 1A), indicating that browning had begun. Pericarp browning was enhanced with prolonged storage. Fruit were out of line with market demands because its appearance became unattractive when the storage period was more than 6 d. The BI, reflecting the browning degree, increased sharply after 3 d of storage and reached a maximum at 6 d (Figure 1B).

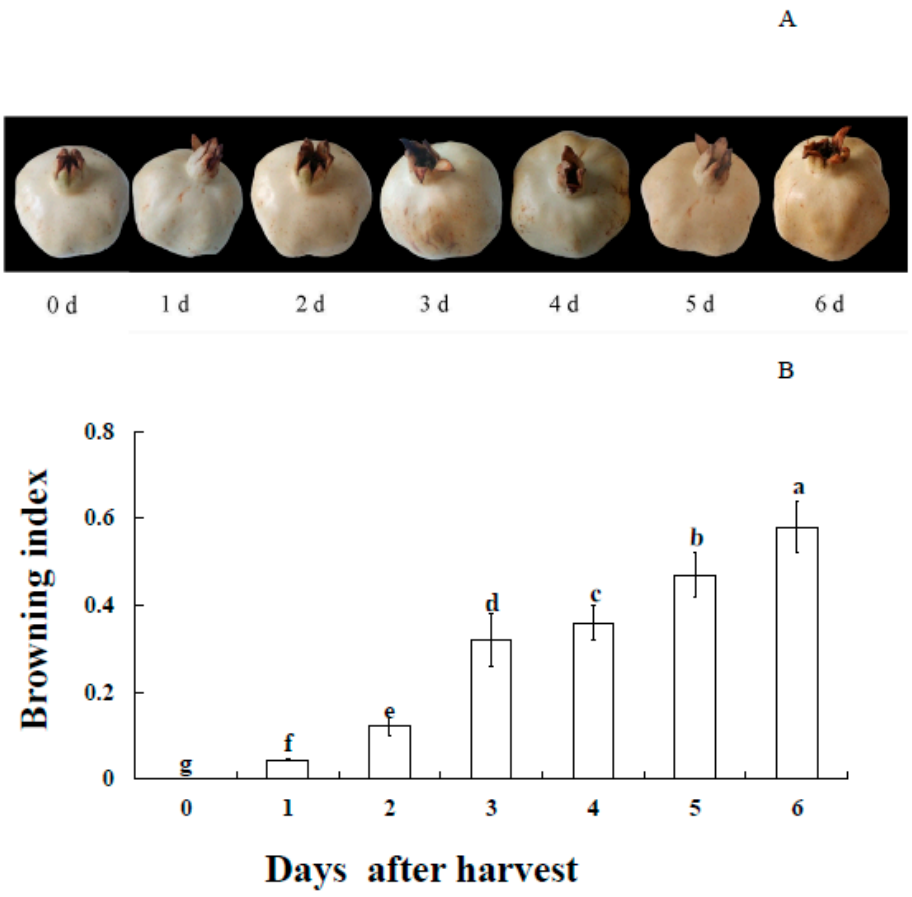

Figure 1. Fruit stored at room temperature (25 ± 2 °C) for 0 to 6 d and the browning index (BI) of pericarp. (**A**) Fruit stored at room temperature (25 ± 2 °C) for 0 to 6 d. (**B**) Browning index (BI) of pericarp of fruit stored at room temperature (25 ± 2 °C) for 0 to 6 d. Vertical lines represent the standard deviation of the means of three replicates. Different small letters indicate a significant difference at $p < 0.05$.

3.2. MDA Concentration and Electrolyte Leakage of Pericarp of Postharvest Fruit

MDA is a product of lipid peroxidation, and its concentration is always used as an indicator of the structural integrity of the cell membranes. We found that the MDA concentration sharply increased after 3 d during fruit storage (Figure 2A), and the change tendency was consistent with that of BI. The electrolyte leakage change is always used as

an indicator of membrane permeability. Herein, we found that the electrolyte leakage was gradually increased during storage, which reached the maximum for 6 d. The electrolyte leakage for 6 d increased 70.71% compared with control (0 d) (Figure 2B).

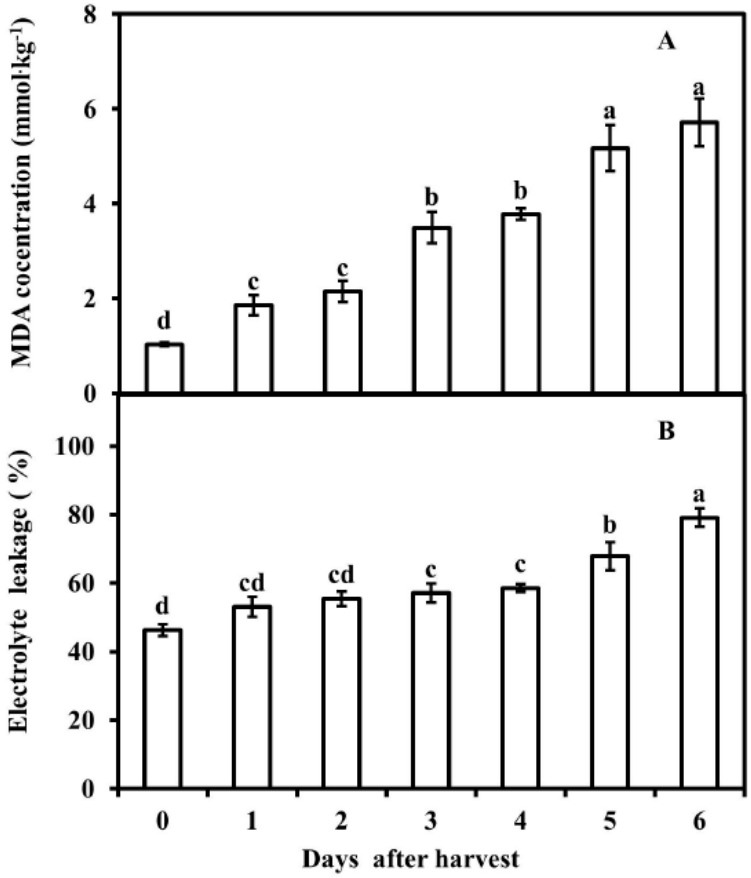

Figure 2. MDA concentration (**A**) and electrolyte leakage (**B**) of pericarp of fruit stored at room temperature (25 ± 2 °C) for 0 to 6 d. Vertical lines represent the standard deviation of the means of three replicates. Different small letters indicate significant difference at $p < 0.05$.

3.3. Activities of Antioxidant Enzymes and Polyphenol Oxidase of Pericarp of Postharvest Fruit

The SOD activity in pericarp of postharvest fruit had a steady slow increase at the early stage of browning; then it declined as the brown color deepened, while the activities of CAT and APX gradually decreased during pericarp browning (Figure 3). Noteworthily, the changing tendency of APX activity was upside down to that of MDA concentration and BI during fruit storage. PPO is an enzyme catalyzing the oxidation of phenolic compounds. There was a great increase in PPO activity at the early stage of pericarp browning, while the increased ratio decreased at the later stage of pericarp browning.

3.4. Antioxidant Substance Contents in Pericarp of Postharvest Fruit

The contents of endogenous antioxidant substances, including GSH and AsA, increased in the early stage of pericarp browning but decreased with the browning deepening (Figure 4). Meanwhile, the content of total phenolic compounds gradually decreased during fruit storage.

3.5. Transcriptome Profiling of Browning Pericarp

A total of approximately 6.69 Gb of reads were generated per sample (Table 1). More than 86.45% of the reads were mapped to the reference genome (https://www.ncbi.nlm.nih.gov/nuccore/MTKT00000000.1/, Accessed on 23 January 2018). An average of 94.27% of the clean reads had Phred quality scores at the Q30 level, indicating a reliable sequencing

quality (Table 1). A total of 6409 DEGs (1352 upregulated and 5057 downregulated, Table S2) between 0 and 6 d (Control vs. RST6) and 4987 DEGs (887 upregulated and 4100 downregulated, Table S2) between Control vs. RTS3 (Figure 5) were identified through comparison.

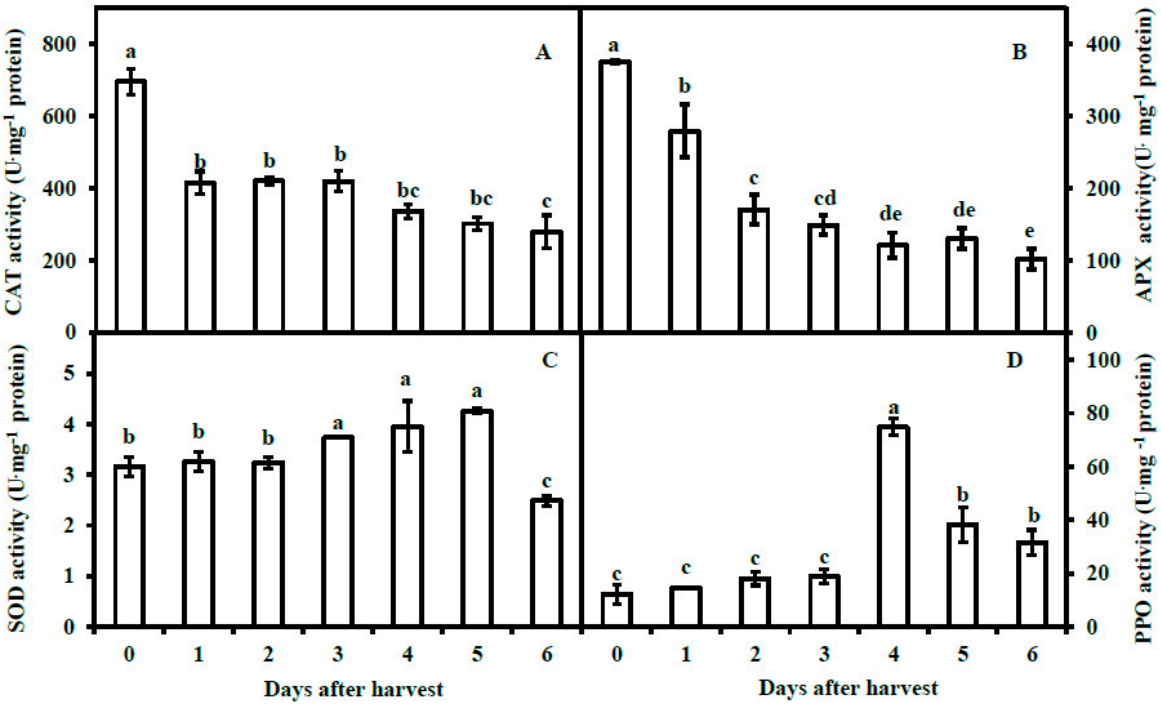

Figure 3. Antioxidase and polyphenol oxidase activity of pericarp of fruit stored at room temperature (25 ± 2 °C) for 0 to 6 d. (**A**), CAT activity; (**B**), APX activity; (**C**), SOD activity; (**D**), PPO activity. Vertical lines represented the standard deviation of the means of three replicates. Different small letters indicated significant difference at $p < 0.05$.

Table 1. Summary of transcriptome of pomegranate pericarp.

Sample	Total Raw Reads (Mb)	Total Clean Reads (Mb)	Total Bases (Gb)	Clean Reads Q30(%)	Total Mapping Ratio (%)
Control_1	55.52	44.12	6.62	94.16	85.07
Control_2	53.88	44.11	6.62	94.29	86.59
Control_3	53.88	44.33	6.65	94.56	86.99
RTS3_1	55.52	44.90	6.74	94.19	87.57
RTS3_2	53.89	44.58	6.69	94.27	88.59
RTS3_3	55.52	45.02	6.75	94.30	86.41
RTS6_1	57.15	45.08	6.76	94.00	83.90
RTS6_2	55.52	44.60	6.69	94.48	85.49
RTS6_3	53.88	44.39	6.69	94.20	87.42

The DEGs were illustrated with a Venn diagram, which showed that 831, 364 and 468 genes were only expressed in the control, RTS3 and RTS6, respectively (Figure 6). The analysis of KEGG was performed with the unique genes in RTS3 (364 genes; Figure 7A) and RTS6 (468 genes; Figure 7B) to identify the potential metabolic pathways that are responsible for the browning of pericarp. We found that the main biological change happened during pericarp browning was metabolism, which including carbohydrate metabolism, the biosynthesis of other secondary metabolites, lipid metabolism, and amino acid metabolism and energy metabolism, besides signal transduction and environmental adaptation.

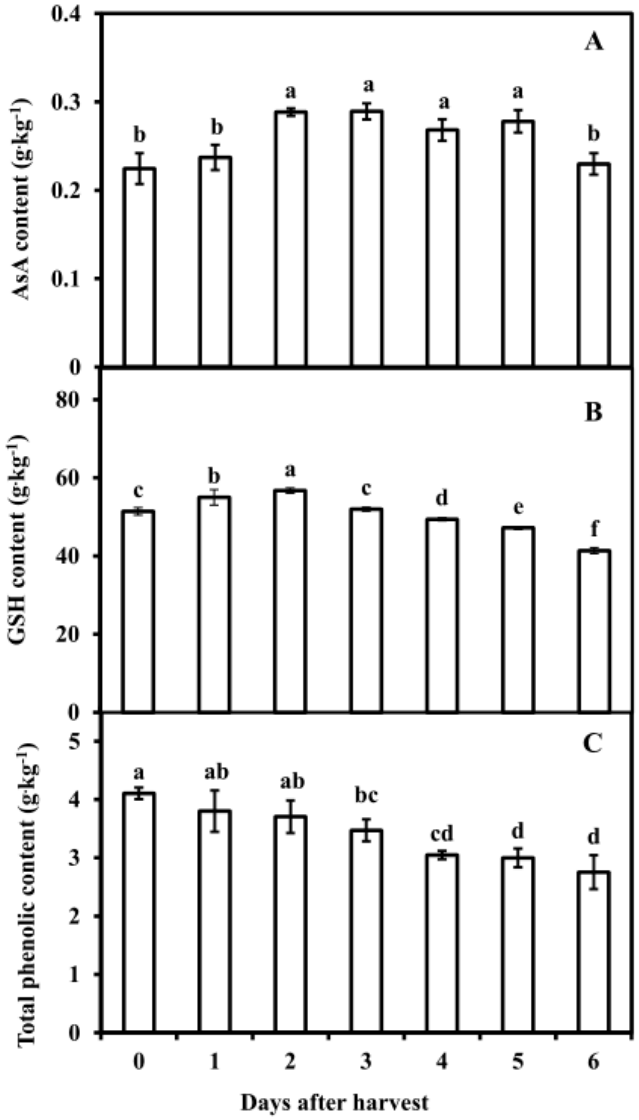

Figure 4. Content of the antioxidant substrates of pericarp of fruit stored at room temperature (25 ± 2 °C) for 0 to 6 d. (**A**), AsA content; (**B**), GSH content; (**C**), Total phenolics content. Vertical lines represented the standard deviation of the means of three replicates. Different small letters indicated significant difference at $p < 0.05$.

3.6. Selection of Candidate Genes Involved in Pericarp Browning

Genes involved in the metabolism of phenolic compounds and ascorbate *Pgr025556* was annotated to PAL, a key enzyme in the biosynthesis of polyphenol compounds, and *Pgr024170* was annotated as POD, an enzyme that catalyzed the oxidation of phenolic compounds to quinones and then condensed tannins to brown polymers. These two genes were continuously upregulated during storage, which was accordant with the fruit browning degree. It is considered that enzymatic browning resulted from the oxidation of phenolic compounds catalyzed by PPO following by the non-enzymatic formation of pigments [36]. In this study, *Pgr016899*, which encoded PPO, had a little bit of a high expression level in browning pericarp (Table 2), meanwhile high PPO activity was detected in pericarp of postharvest fruit, especially for those at the later storage stages (Figure 3D). This implied that PPO may contribute to the development of brown pigments.

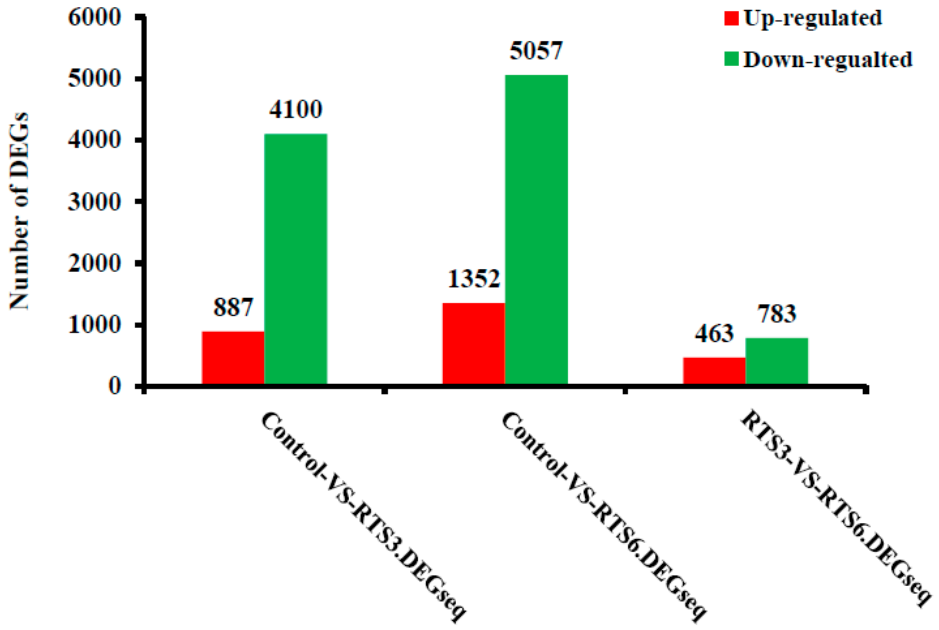

Figure 5. Numbers of regulated genes in browning pericarp. Red columns represent the numbers of upregulated genes, and green columns represent the numbers of downregulated genes.

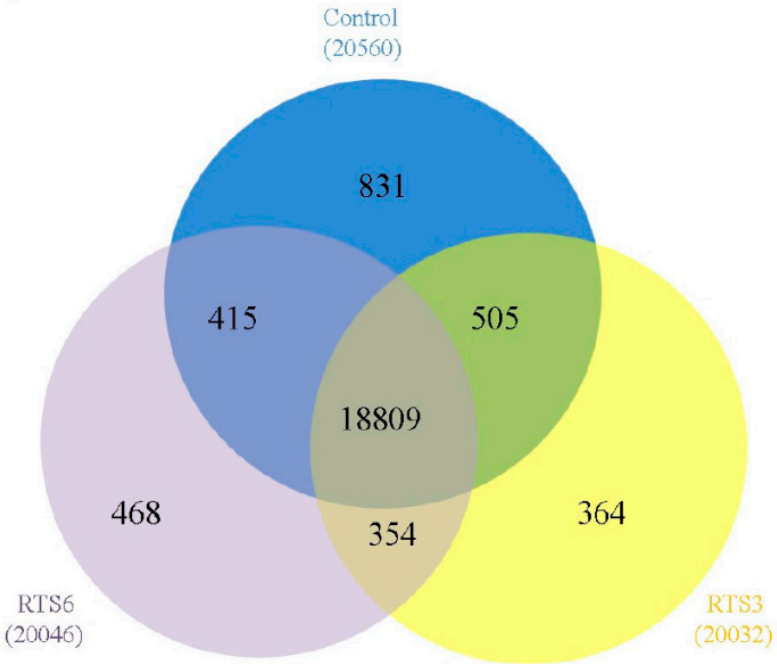

Figure 6. Venn diagram of transcripts in pomegranate pericarp. Control, RTS3 and RTS6 represent the pericarp of fruit stored for 0, 3 and 6 d.

Furthermore, the correlation between enzymatic browning and the accumulation of reactive oxygen species (ROS) were confirmed [6,37,38]. SOD, CAT and APX, the key enzymes scavenging H_2O_2 and superoxide, can scavenge ROS and prevent the accumulation of ROS [8], then the reduced membrane lipid peroxidation and the reduction in pericarp browning were confirmed in harvested litchi fruit [39]. In pomegranate, the reduced expression of *Pgr020281* and *Pgr020981* (encoding SOD), *Pgr014250* (encoding CAT), and *Pgr025048* and *BGI_novel_G000299* (encoding APX) were detected during pericarp browning (Table 2). Besides, there is a non-enzymatic active oxygen scavenging system, which contains endogenous antioxidant substances like AsA and GSH [8], and the overall capacity

of scavenging ROS is closely related to the contents of AsA and GSH [40]. The downregulated *Pgr019084*, a gene encoding L-galactono-1,4-lactone dehydrogenase (L-GalLDH), and *Pgr026685*, a gene encoding L-ascorbate oxidase (AOX) and involved in the irreversible oxidization of AsA, were detected in browning pericarp (Table 2). Meanwhile, reduced contents of AsA and GSH were also detected in the brown pericarp. This implied that non-enzymatic browning accompanied the enzymatic browning occurred in the pericarp.

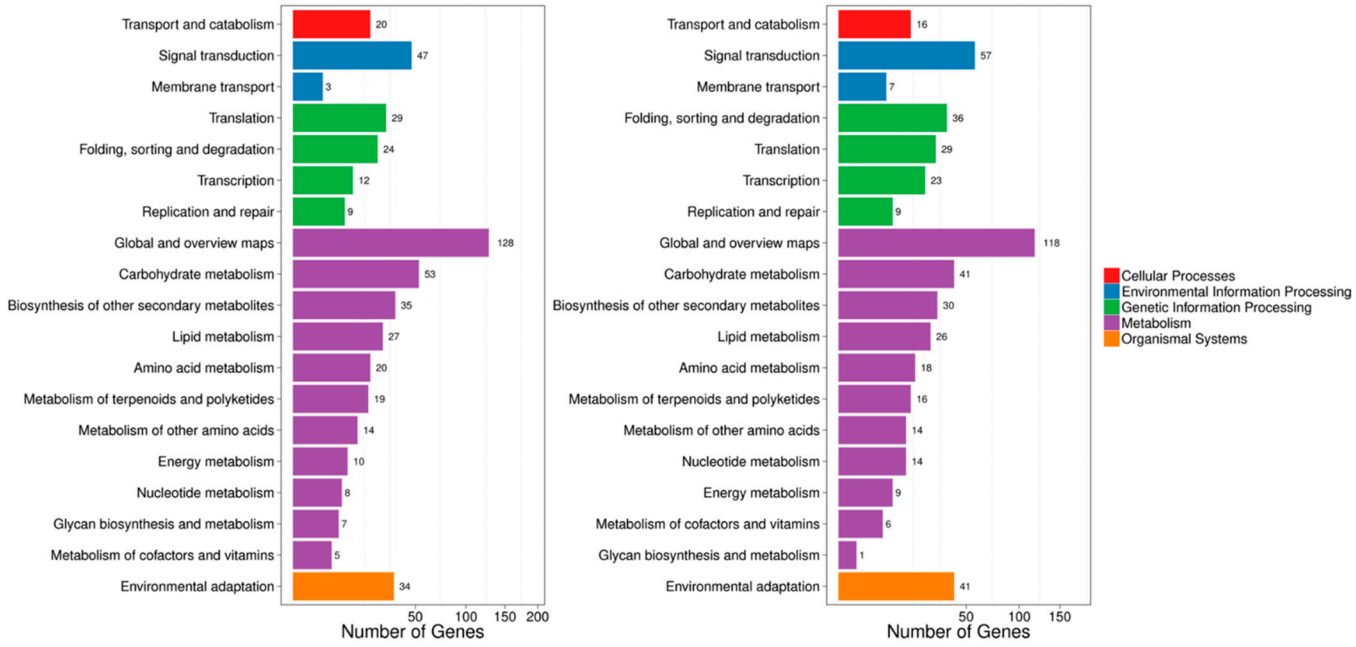

Figure 7. KEGG enrichment of genes only expressed in RTS3 (**A**) and RTS6 (**B**). The *X*-axis is the number of genes. The *Y*-axis is the functional classification of KEGG (Kyoto Encyclopedia of Genes and Genomes).

Table 2. List of genes potentially related with pericarp browning of pomegranate.

Gene ID	Length (bp)	FPKM			Gene Description
		Control	RTS3	RTS6	
Genes encode enzymes involved in phenolic compound metabolism					
Pgr016899	2849	26.42	26.31	33.04	polyphenol oxidase
Pgr024170	1086	0.02	0.18	0.38	peroxidase
Pgr025556	2687	93.05	184.02	328.36	phenylalanine ammonia-lyase
Genes involved ascorbic acid-glutathione metabolism and encoding antioxidant enzymes					
Pgr019084	2443	27.85	12.23	12.63	L-galactono-1,4-lactone dehydrogenase
Pgr026685	1317	0.34	0	0.02	L-ascorbate oxidase
Pgr020281	1704	49.92	10.01	8.87	copper/zinc superoxide dismutase
Pgr020981	1471	8.92	3.04	3.36	superoxide dismutase [Fe] 3
Pgr014250	1917	3467.51	1691.19	1540.47	catalase isozyme 3
Pgr025048	1365	310.49	122.97	95.11	L-ascorbate peroxidase 2, cytosolic
BGI_novel_G000299	1128	1.95	0.66	0.63	PREDICTED: putative L-ascorbate peroxidase 6 isoform X8
Genes involved in energy-related pathway					
Pgr016265	729	25.67	14.94	9.47	NADH dehydrogenase (ubiquinone) activity
Pgr016267	873	18.94	7.75	4.06	NADH dehydrogenase (ubiquinone) activity
Pgr013991	1234	147.68	85.29	74.04	ATP synthase, mitochondrial
Pgr012837	1041	26.78	48.72	38.53	alternative oxidase activity

Table 2. *Cont.*

Gene ID	Length (bp)	FPKM			Gene Description
		Control	RTS3	RTS6	
Pgr009832	1413	444.53	189.83	212.89	glyceraldehyde 3-phosphate dehydrogenase
Pgr022301	1616	218.53	68.49	45.48	glyceraldehyde 3-phosphate dehydrogenase
Pgr007501	1035	193.95	64.26	42.07	malate dehydrogenase, mitochondrial
Pgr002381	1050	102.24	43.67	43.29	malate dehydrogenase, mitochondrial
Pgr017364	1627	2.47	0.46	0.19	alcohol dehydrogenase 1
BGI_novel_G000840	1471	1.19	0.41	0.65	alcohol dehydrogenase 1 isoform X2
Pgr009655	2284	58.94	23.29	15.28	pyruvate dehydrogenase E1 component alpha subunit
Pgr002364	3888	43.74	14.12	8.95	phosphoenolpyruvate carboxylase, housekeeping isozyme
Pgr024145	4230	27.76	12.64	13.8	phosphoenolpyruvate carboxylase 4
Genes involved in lipid metabolism					
Pgr027677	2583	0.13	0.3	0.5	phospholipase D
Pgr013780	2754	50.9	60.16	82.13	lipoxygenase
Genes involved in sugar and starch metabolism					
Pgr009313	3111	57.36	97.78	163.44	sucrose synthase
Pgr008953	1905	28.3	13.11	10.76	ADP-glucose pyrophosphorylase family protein
Pgr018115	2529	111.59	45.33	50.01	granule-bound starch synthase
Genes involved ethylene biosynthesis and signal transduction					
Pgr012839	1349	14.7	0.22	0.04	1-aminocyclopropane-1-carboxylate oxidase
Pgr011853	1173	4.11	0.47	0.65	1-aminocyclopropane-1-carboxylate oxidase
Pgr012022	1763	10.41	65.17	58.36	ethylene-responsive transcription factor
Pgr013421	1199	0.44	0.95	1.64	AP2-like ethylene-responsive transcription factor

Note: The FPKM values are means of three independent biological replications.

3.6.1. Genes Involved in Energy-Related Pathways

The decline of ATP levels and energy charge in postharvest fruit caused a disruption in energy metabolism [41]. Energy deficiency of browning fruit was characterized due to decreased energy synthesis [42]. Several genes encoding enzymes involving in energy synthesis were differentially expressed in postharvest pomegranate fruit. The expression of *Pgr016265* and *Pgr016267*, two genes encoding NADH dehydrogenase (NDA), had a rapid decrease from 0 to 3 d after harvest (Table 2). The expression of *Pgr013991*, which encoded ATP synthase (ATPase), an enzyme involved in the oxidative phosphorylation pathway sharply deceased from 0 d to 3 d after harvest but showed a minor decrease from 3 d to 6 d after harvest. There is evidence indicating that AOX is controlled by the redox status, which has an impact on ATP production [43]. The transcript amount of *Pgr012837*, a gene encoding AOX, was 1.82-fold and 1.43-fold higher in RTS3 and RTS6, respectively, than in control (0 d).

Furthermore, several genes involved in the tricarboxylic acid (TCA) cycle, which is at the crossroads of substrate oxidation, respiration and free radical generation, had rhythmic transcript accumulation during browning. These genes included *Pgr009832* and *Pgr022301*, *Pgr007501* and *Pgr002381*, *Pgr017364* and *BGI_novel_G000840*, *Pgr009655*, *Pgr002364* and *Pgr024145*.

3.6.2. Genes Involved in Lipid Metabolism

Increased MDA concentration is the result of lipid peroxidation, degrading enzymes, such as phospholipase D (PLD) and lipoxygenase (LOX), involved in the process [44]. In the pericarp of postharvest pomegranate fruit, the expression of *Pgr027677* was gradually upregulated during storage (Table 2), while the expression level of *Pgr013780* increased promptly during browning and reached the maximum level in RTS6 compared with control (0 d).

3.6.3. Genes Involved in Sugar and Starch Metabolism

Fruit browning depends on non-enzymatic reactions, as well as enzymatic processes. The increased content of reducing sugar was detected in pomegranate pericarp at later storage stages [21], which may cause cell membrane oxidative stress accompanied by browning. The transcripts of *Pgr009313* (encoding SuSy) were increased, while the transcripts of *Pgr008953* and *Pgr018115*, two genes involving in starch synthase, were decreased during the pericarp browning of pomegranate (Table 2). The decreased expression of *Pgr008953* and *Pgr018115* indicated that starch biosynthesis might be suppressed by the saturation of starch grains within cells.

3.6.4. Genes Involved in Ethylene Biosynthesis and Signal Transduction

Increased ethylene production, as well as enhanced amounts of PPO and substrates for the browning reaction, contributed to the fruit browning [45]. The expression of the *Pgr012839* and *Pgr011853* (annotated as aminocyclopropane-1-carboxylic oxidase, an enzyme involving in ethylene biosynthesis) was higher in the control, which might trigger initial ethylene biosynthesis (Table 2). The expression of *Pgr012022* and *Pgr013421* were increased in RTS3 and RTS6 compared to the control. The results suggested that ethylene might play some role in the pericarp browning of pomegranate fruit.

To confirm the reliability of the results of transcriptome sequencing, six candidate genes involving in multiple metabolic pathways were selected to investigate the relative expression levels by qRT-PCR. The relative expression of *Pgr025556* and *Pgr009313* was significantly increased during pericarp browning, while the relative expression of *Pgr020281* and *Pgr013991* was significantly decreased during pericarp browning. Meanwhile, the increased expression of *Pgr016899* and *Pgr013780* was detected in the browning pericarp (Figure 8). This revealed that the results of qRT-PCR were generally accordant with that of RNA-seq, and the Pearson correlation coefficient index was 0.78 to 0.97, which implied that the candidate genes selected based on the RNA-seq were reliable for accounting for the mechanism of pericarp browning.

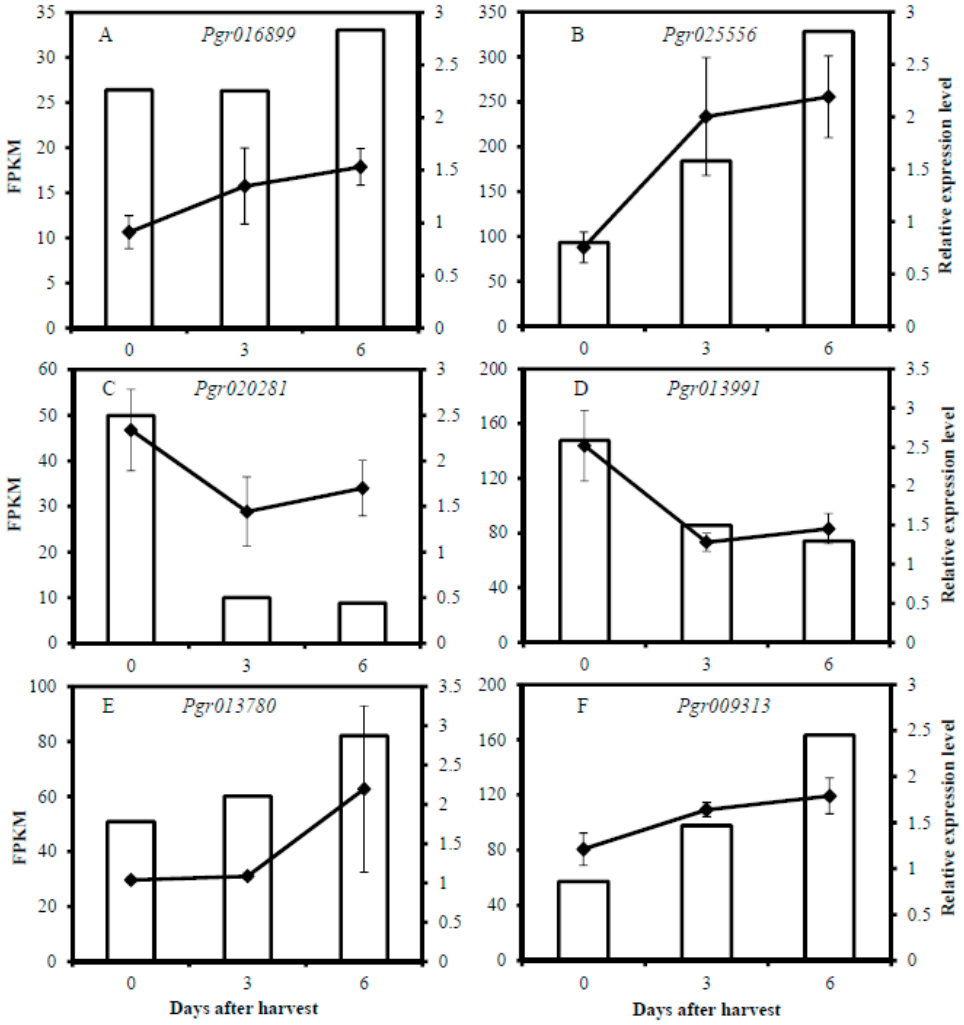

Figure 8. Relative expression levels of candidate genes by qRT-PCR and transcript amounts of candidate genes. The left y-axis is the result of RNA-seq (white histogram). The right y-axis is the relative expression level determined by qRT-PCR (black lines). The genes and their encoding enzymes are the following, (**A**) *Pgr016899*, polyphenol oxidase; (**B**) *Pgr025556*, phenylalanine ammonia-lyase; (**C**) *Pgr020281*, superoxide dismutase; (**D**) *Pgr013991*, ATP synthase; (**E**) *Pgr013780*, lipoxygenase and (**F**) *Pgr009313*, sucrose synthase. Vertical bars represented the standard deviation of the means of three replicates.

4. Discussion

'Baiyushizi' pomegranate is a popular fresh fruit in the Anhui province of China, due to its desirable flavor and attractive appearance. However, brown pericarp on postharvest fruit greatly affected fruit appearance and marketability. A study on the physiological and genetic mechanism of pericarp browning would be appealing for controlling the browning of pomegranate pericarp. The decreased SOD, CAT and APX activity and the reduction in the amounts of endogenous antioxidant substances in pericarp of postharvest fruit indicated a decrease of active oxygen-scavenging, which could result in the reduced ability of scavenging ROS or enhanced ROS accumulation. Furtherly, it promoted lipid peroxidation and the breakdown of the structural integrity of cellular membrane. Meanwhile, the increased activity of PPO might accelerate the brown polymer accumulation. Thereby, pericarp browning occurred, and the appearance lost attractiveness.

The transcriptome profiling of pericarp from 0 d (control), 3 d (RTS3) and 6 d (RTS6) revealed that genes involved in carbohydrate metabolism, the biosynthesis of other secondary metabolites, lipid metabolism, amino acid metabolism and energy metabolism

might contribute to pericarp browning. The accumulation of gene transcripts associated with the oxidation of phenolic compounds is a hallmark of enzymatic browning. Many studies have confirmed that the browning-related genes differentially expressed in browning in harvested horticultural crops were associated with the metabolism of phenolic compounds [46,47]. Elfalleh et al. [48] considered that pomegranate pericarp browning is generally attributable to the oxidation of secondary metabolites, including phenolic compounds. The compounds were productions of phenolic metabolism, which was catalyzed by PPO, PAL and so on [49,50]. PAL catalyzes the conversion of L-phenylalanine to trans-cinnamic acid and ammonia. It has been shown to be a key enzyme in the biosynthesis of polyphenol compounds, which could be oxidized by PPO to form browning pigments in damaged plant tissues [51]. Thus, increased transcripts of *Pgr025556* (PAL) and *Pgr016899* (PPO) in browning pericarp may be indicative of their role in pericarp browning. Similar transcriptome patterns of POD and PAL in browning pericarp was also found in luffa, wherein the expression levels of PPO, POD and PAL were higher in a browning-sensitive cultivar than in a browning-resistant cultivar [52]. Several other genes associated with oxidoreductase processes (respiratory burst oxidase and the ascorbate–glutathione cycle) were also differentially regulated in browning pomegranate pericarp (Table 2). The remarkably decreased activities of protective enzymes included SOD, CAT and APX (Figure 3), and the reduced transcripts accumulation of genes encoding SOD, CAT and APX were detected in browning pomegranate pericarp. The regulated expression of genes encoding antioxidant enzymes may contribute to the accumulation of ROS that causes the loss of membrane integrity and functionality [53], although cell membrane damage during fruit browning might also be related to energy deficit [54]. In the present study, gene transcripts for NDA and ATPase, which are involved in energy, were downregulated during the storage processes. Furthermore, transcripts of several genes involved in the TCA cycle were also reduced during storage. The dynamic changes in the expression of these genes indicated that the pericarp browning may be caused by decreased cellular energy level and restricted the utilization of energy in pomegranate fruit, just as what happened in harvested longan fruits [52]. Furthermore, the gene expression levels of PLD and LOX were higher in RTS6 compared with control (0 d), suggesting that the deterioration of membrane integrity and the loss of compartmentation gives rise to accelerated browning.

The browning of fruit and vegetables is not only dependent on enzymatic processes but also undergoes many non-enzymatic reactions. Several complexes of different chemical reactions and carbonylic intermediates were involved in non-enzymatic reactions [55]. The Maillard reaction is a form of non-enzymatic browning reaction commonly associated with reducing sugars and compounds of the free amino groups of amino acids or proteins [56]. Korbel et al. [57] reported that reducing sugar participated in the non-enzymatic browning of mango during drying, partly accounting for the role of reducing sugar for browning reactions. The increased *Pgr009313* transcripts (Table 2) and consequently increased reducing sugar content [21] during the later period of storage were detected in the browning pericarp of pomegranate. However, the decreased expression of *PgrAGPase* and *PgrGBSS* indicated that starch biosynthesis might have been suppressed by the saturation of starch grains within cells [58].

It was reported that the expression of genes involved in ethylene biosynthesis and signal transduction was responsible for fruit browning [17,59]. In our transcriptomic analysis, two ACO genes were downregulated during storage, while an ERF gene and another gene encoding AP2-like ethylene-responsive transcription factor were upregulated during the storage. These results indicated that ethylene could play a role in the pericarp browning of harvested pomegranate fruit.

An outline of major metabolic pathways or related processes of browning pericarp was sketched according to the physiological change and expression pattern of DEGs for postharvest fruit (Figure 9). Enzymatic and non-enzymatic browning reactions of amino acids and proteins with carbohydrates, oxidized lipids and oxidized phenolics comprehensively cause the deterioration of pericarp in pomegranate during storage. Enzymatic browning

comprises the enzymatic oxidation of phenolic substrates and the subsequent oxidation of phenolic compounds to form brown polymers. Non-enzymatic browning causes oxidative stress and changes in cellular metabolism from the respiratory to the metabolic pathways, which are less energy-efficient, so that insufficient energy becomes available for normal maintenance processes and the repair of membrane damage by ROS. This may lead to the production of less energy and damage to the function and compartmentalization of the cell membrane. The decreased expression of a series of genes encoding enzymes involved in energy metabolism may result in a decrease of ATPase, NADH dehydrogenase activity and available ATP, then break the ion homeostasis and the integrity of mitochondria. Meanwhile, some genes that are involved in TCA cycle, lipid metabolism, sugar and starch metabolism may be also repressed in the browning processes. During the course of pericarp browning, genes encoding SOD, CAT and APX, which are involved in the antioxidant system were downregulated; then there was a consequent decrease in SOD, CAT, and APX activity, serving as a generic weakened defense response in plants. In addition, genes involving in ethylene biosynthesis and signal transduction were affected in the pericarp browning of pomegranate. The high expression levels of genes coding ERF and AP2, two ethylene-responsive related genes in pomegranates, indicated that increased ethylene level may aggravate the pericarp browning in harvested fruit.

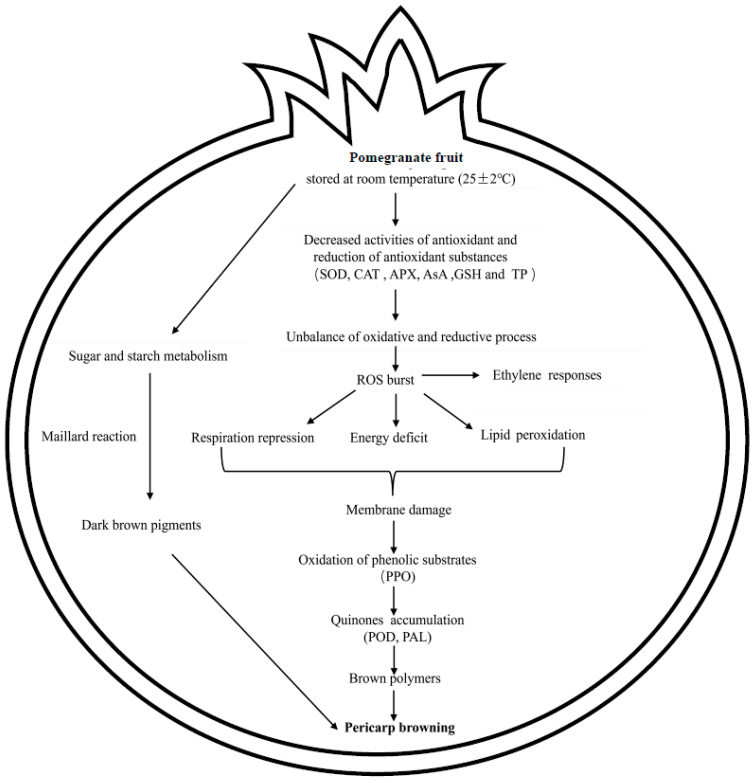

Figure 9. A Schematic of the pericarp browning of pomegranate fruit. Abbreviation: ROS, reactive oxygen species; SOD, superoxide dismutase; CAT, catalase; APX, ascorbate peroxidases; AsA, ascorbic acid; GSH, glutathione; TP, total phenolics; PPO, polyphenol oxidase; POD, peroxidase; PAL, phenylalanine ammonia lyase.

5. Conclusions

Pericarp browning obviously occurred in the fruit of the browning-sensitive cultivar 'Baiyushizi' after 3 d storage at room temperature. The marketability of fruit lost after 6 d storage or more. Reduced activities of antioxidant enzymes including SOD, CAT and APX and the reduction of antioxidant substances including GSH, AsA and total phenolics were detected in the pericarp of postharvest fruit. Furthermore, increased MDA concentration and electrolyte leakage, indicators of lipid peroxidation and membrane permeability, were

detected in browning pericarp. The genome-wide transcriptome profiling of pericarp provided key information on the molecular mechanisms of pericarp browning. Candidate genes that potentially contributed to pericarp browning, included those involved in phenolic oxidation, energy-related pathways, lipids, the ascorbic-acid–glutathione cycle, carbohydrate and hormone metabolism, and ethylene-response were identified. Putative metabolic pathways and processes that contributed to pericarp browning were described based on the results from physiological changes and DEGs in browning pericarp. The information not only helps us better understand the underlying biology of pericarp browning in pomegranate but also provides insights to controlling pericarp browning.

Supplementary Materials: The following supporting information can be downloaded at: https://www.mdpi.com/article/10.3390/horticulturae8100924/s1, Figure S1: Samples of exocarp tissues were dissected from fruit hip, Table S1: Primers for real-time PCR, Table S2: Differentially expressed genes between 0 and 6 d (Control vs. RST6), Table S3: Differentially expressed genes between 0 and 3 d (Control vs. RTS3).

Author Contributions: G.Q. and Y.X. conceived the project. X.Q. and J.Z. analyzed the bioinformatics data and drafted the manuscript. X.Q., Y.S., C.H. and Z.C. performed qRT-PCR. C.L. and J.L. took part in the interpretation of the results. G.Q., Z.J. and Y.P. revised the manuscript. All authors have read and agreed to the published version of the manuscript.

Funding: This work was supported by the Excellent Young Talents Fund Program of Higher Education Institutions of Anhui Province, China (gxyq2020072); Natural Science Research Project of University of Anhui Province (KJ2021A1254); and the Special Project on Science and Technology of Anhui Province, China (201903b06020017).

Institutional Review Board Statement: Not applicable.

Informed Consent Statement: Not applicable.

Data Availability Statement: The RNA-seq data have been deposited in the NCBI Sequence Read Archive under accession number PRJNA610913.

Conflicts of Interest: The authors declare no conflict of interests.

References

1. Seeram, N.P.; Schulman, R.N.; Heber, D. *Pomegranates: Ancient Roots to Modern Medicine*; CRC Press: Boca Raton, FL, USA, 2006; pp. 63–183.
2. Qin, G.H.; Xu, C.Y.; Ming, R.; Tang, H.B.; Guyot, R.; Kramer, E.M.; Hu, Y.D.; Yi, X.K.; Qi, Y.J.; Xu, X.Y.; et al. The pomegranate (*Punica granatum* L.) genome and the genomics of punicalagin biosynthesis. *Plant J.* **2017**, *91*, 1108–1128. [CrossRef]
3. Ioannou, I.; Ghoul, M. Prevention of enzymatic browning in fruit and vegetables. *Eur. J. Sci.* **2013**, *9*, 310–341. [CrossRef]
4. Wei, W.L.; Xu, C.; Wu, L.; Wang, J.S.; Ren, J.S.; Qu, X.G. Non-enzymatic-browning-reaction: A versatile route for production of nitrogen-doped carbon dots with tunable multicolor luminescent display. *Sci. Rep.* **2014**, *4*, 3564. [CrossRef] [PubMed]
5. Hong, P.K.; Betti, M. Non-enzymatic browning reaction of glucosamine at mild conditions: Relationship between colour formation, radical scavenging activity and α-dicarbonyl compounds production. *Food Chem.* **2016**, *212*, 234–243. [CrossRef] [PubMed]
6. Sun, J.Z.; Lin, H.T.; Zhang, S.; Lin, Y.F.; Wang, H.; Lin, M.S.; Hung, Y.C.; Chen, Y.H. The roles of ROS production-scavenging system in *Lasiodiplodia theobromae* (Pat.) Griff. & Maubl.-induced pericarp browning and disease development of harvested longan fruit. *Food Chem.* **2018**, *247*, 16–22. [CrossRef]
7. Ali, S.; Khan, A.S.; Nawaz, A.; Anjum, M.A.; Naz, S.; Ejaz, S.; Hussain, S. Aloe vera gel coating delays postharvest browning and maintains quality of harvested litchi fruit. *Postharvest Biol. Technol.* **2019**, *157*, 110960. [CrossRef]
8. Lin, Y.F.; Lin, H.T.; Zhang, S.; Chen, Y.H.; Chen, M.Y.; Lin, Y.X. The role of active oxygen metabolism in hydrogen peroxide-induced pericarp browning of harvested longan fruit. *Postharvest Biol. Technol.* **2014**, *96*, 42–48. [CrossRef]
9. Lamikanra, O.; Watson, M.A. Effects of ascorbic acid on peroxidase and polyphenoloxidase activities in fresh-cut cantaloupe melon. *J. Food Sci.* **2001**, *66*, 1283–1286. [CrossRef]
10. Degl'Innocenti, E.; Pardossi, A.; Tognoni, F.; Guidi, L. Physiological basis of sensitivity to enzymatic browning in 'lettuce', 'escarole' and 'rocket salad' when stored as fresh-cut products. *Food Chem.* **2007**, *104*, 209–215. [CrossRef]
11. Holderbaum, D.F.; Kon, T.; Kudo, T.; Guerra, M.P. Enzymatic browning, polyphenol oxidase activity, and polyphenols in four apple cultivars: Dynamics during fruit development. *HortScience* **2010**, *45*, 1150–1154. [CrossRef]
12. Banerjee, A.; Suprasanna, P.; Variyar, S.; Sharma, A. Gamma irradiation inhibits wound induced browning in shredded cabbage. *Food Chem.* **2015**, *173*, 38–44. [CrossRef]

13. Zhu, H.S.; Liu, J.T.; Wen, Q.F.; Chen, M.D.; Wang, B.; Zhang, Q.R.; Xue, Z.Z. De novo sequencing and analysis of the transcriptome during the browning of fresh cut *Luffa cylindrica* 'Fusi-3' fruit. *PLoS ONE* **2017**, *12*, e0187117. [CrossRef]
14. Ali, S.; Nawaz, A.; Ejaz, S.; Haider, S.T.A.; Alam, M.W.; Javed, H.U. Effects of hydrogen sulfide on postharvest physiology of fruits and vegetables: An overview. *Sci. Hortic.* **2019**, *243*, 290–299. [CrossRef]
15. Zhang, Z.; Huber, D.J.; Qu, H.; Yun, Z.; Wang, H.; Huang, Z.; Huang, H.; Jiang, Y. Enzymatic browning and antioxidant activities in harvested litchi fruit as influenced by apple polyphenols. *Food Chem.* **2015**, *171*, 191–199. [CrossRef] [PubMed]
16. Chi, M.; Bhagwat, B.; Lane, W.D.; Tang, G.L.; Su, Y.G.; Sun, R.; Oomah, B.D.; Wiersma, P.A.; Xiang, Y. Reduced polyphenol oxidase gene expression and enzymatic browning in potato (*Solanum tuberosum* L.) with artificial microRNAs. *BMC Plant Biol.* **2014**, *14*, 62. [CrossRef]
17. Liu, P.; Xue, C.; Wu, T.T.; Heng, W.; Jia, B.; Ye, Z.F.; Liu, L.; Zhu, L.W. Molecular analysis of the processes of surface brown spot (SBS) formation in pear fruit (*Pyrus bretschneideri* Rehd. Cv. Dangshansuli) by de novo transcriptome assembly. *PLoS ONE* **2013**, *8*, e74217. [CrossRef] [PubMed]
18. Chen, X.; Tan, T.M.; Xu, C.C.; Huang, S.P.; Tan, J.; Zhang, M.; Wang, C.L.; Xie, C.H. Genome-wide transcriptome profiling reveals novel insights into *Luffa cylindrica* browning. *Biochem. Biophys. Res. Commun.* **2015**, *463*, 1243–1249. [CrossRef]
19. Zhang, Y.L.; Zhang, R.G. Study on the mechanism of browning of pomegranate (*Punica granatum* L. cv. Ganesh) peel in different storage conditions. *Agric. Sci. China* **2008**, *7*, 65–73. [CrossRef]
20. Feng, L.J.; Yin, Y.L.; Yang, X.M.; Wang, C.Z.; Jiao, Q.Q. Changes of browning and its related enzyme activities in pomegranate peel during fruit development period. *J. Nucl. Agric. Sci.* **2017**, *31*, 821–827. (In Chinese) [CrossRef]
21. Qi, X.X.; Qin, G.H. Study on the factors influencing postharvest browning of the pomegranate peel. *J. Fruit Sci.* **2017**, *34*, 735–743. (In Chinese) [CrossRef]
22. Sun, J.; You, X.R.; Li, L.; Peng, H.X.; Su, W.Q.; Li, C.B.; He, Q.G.; Liao, B. Effects of a phospholipase D inhibitor on postharvest enzymatic browning and oxidative stress of litchi fruit. *Postharvest Biol. Technol.* **2011**, *62*, 288–294. [CrossRef]
23. Zhu, L.Q.; Zhou, J.; Zhu, S.H.; Guo, L.H. Inhibition of browning on the surface of peach slices by short-term exposure to nitric oxide and ascorbic acid. *Food Chem.* **2009**, *114*, 174–179. [CrossRef]
24. Cao, J.K.; Jiang, W.B.; Zhao, Y.M. *Experiment Guidance of Postharvest Physiology and Biochemistry of Fruits and vegetables*; China Light Industry Press: Beijing, China, 2007; pp. 101–103.
25. Zhang, R.G.; Guo, X.C.; Zhang, Y.L.; Tian, C.R. Influence of modified atmosphere treatment on post-harvest reactive oxygen metabolism of pomegranate peels. *Nat. Prod. Res.* **2018**, *34*, 740–744. [CrossRef] [PubMed]
26. Wojdyło, A.; Oszmiański, J.; Bielicki, P. Polyphenolic composition, antioxidant activity, and polyphenol oxidase (PPO) activity of quince (*Cydonia oblonga* Miller) varieties. *J. Agric. Food Chem.* **2013**, *61*, 2762–2772. [CrossRef] [PubMed]
27. Bradford, M.M. A rapid and sensitive method for the quantitation of microgram quantities of protein utilizing the principle of protein-dye binding. *Anal. Biochem.* **1976**, *72*, 248–254. [CrossRef]
28. Cai, Y.T.; Cao, S.F.; Yang, Z.F.; Zheng, Y.H. MeJA regulates enzymes involved in ascorbic acid and glutathione metabolism and improves chilling tolerance in loquat fruit. *Postharvest Biol. Technol.* **2011**, *59*, 324–326. [CrossRef]
29. Li, L.; Zhang, Y.Y.; Fan, X.L.; Wang, J.D.; Liang, L.Y.; Yan, S.J.; Xiao, L.X. Relationship between activated oxygen metabolism and browning of "Yali" pears during storage. *J. Food Process. Preserv.* **2020**, *44*, e14392. [CrossRef]
30. Ainsworth, E.A.; Gillespie, K.M. Estimation of total phenolic contents and other oxidation substrates in plant tissue using Folin-Ciocalteu reagent. *Nat. Protoc.* **2007**, *2*, 875–877. [CrossRef]
31. Kumar, R.; Ichihashi, Y.; Kimura, S.; Chitwood, D.H.; Headland, L.R.; Peng, J.; Maloof, J.N.; Sinha, N.R. A high-throughput method for Illumina RNA-Seq library preparation. *Front. Plant Sci.* **2012**, *3*, 202. [CrossRef]
32. Kim, D.; Langmead, B.; Salzberg, S.L. HISAT: A fast spliced aligner with low memory requirements. *Nat. Methods* **2015**, *12*, 357–360. [CrossRef]
33. Langmead, B.; Salzberg, S. Fast gapped-read alignment with Bowtie 2. *Nat. Methods* **2012**, *9*, 357–359. [CrossRef] [PubMed]
34. Li, B.; Dewey, C.N. RSEM: Accurate transcript quantification from RNA-Seq data with or without a reference genome. *BMC Bioinform.* **2011**, *12*, 323. [CrossRef]
35. Wang, L.K.; Feng, Z.X.; Wang, X.; Wang, X.W.; Zhang, X.G. DEGseq: An R package for identifying differentially expressed genes from RNA-seq data. *Bioinformatics* **2010**, *26*, 136–138. [CrossRef] [PubMed]
36. He, Q.; Luo, Y.G. Enzymatic browning and its control in fresh-cut produce. *Stewart Postharvest Rev.* **2007**, *3*, 1–7. [CrossRef]
37. Chumyam, A.; Faiyue, B.; Saengnil, K. Reduction of enzymatic browning of fresh-cut guava fruit by exogenous hydrogen peroxide-activated peroxiredoxin/thioredoxin system. *Sci. Hortic.* **2019**, *255*, 260–268. [CrossRef]
38. Tang, T.T.; Xie, X.F.; Ren, X.; Wang, W.J.; Tang, X.M.; Zhang, J.; Wang, Z.D. A difference of enzymatic browning unrelated to PPO from physiology, targeted metabolomics and gene expression analysis in Fuji apples. *Postharvest Biol. Technol.* **2020**, *170*, 111323. [CrossRef]
39. Duan, X.W.; Liu, T.; Zhang, D.; Su, X.G.; Lin, H.T.; Jiang, Y.M. Effect of pure oxygen atmosphere on antioxidant enzyme and antioxidant activity of harvested litchi fruit during storage. *Food Res. Int.* **2011**, *44*, 1905–1911. [CrossRef]
40. Silva, V.L.D.; Cerqueira, M.R.F.; Lowinsohn, D.; Matos, M.A.C.; Matos, R.C. Amperometric detection of ascorbic acid in honey using ascorbate oxidase immobilised on amberlite IRA-743. *Food Chem.* **2012**, *133*, 1050–1054. [CrossRef]
41. Wang, Y.S.; Luo, Z.S.; Khan, Z.U.; Mao, L.C.; Ying, T.J. Effect of nitric oxide on energy metabolism in postharvest banana fruit in response to chilling stress. *Postharvest Biol. Technol.* **2015**, *108*, 21–27. [CrossRef]

42. Wang, J.W.; Jiang, Y.G.; Li, G.D.; Lv, M.; Zhou, X.; Zhou, Q.; Fu, W.W.; Zhang, L.; Chen, Y.F.; Ji, S.J. Effect of low temperature storage on energy and lipid metabolisms accompanying peel browning of 'Nanguo' pears during shelf life. *Postharvest Biol. Technol.* **2018**, *139*, 75–81. [CrossRef]
43. Saha, B.; Borovskii, G.; Panda, S.K. Alternative oxidase and plant stress tolerance. *Plant Signal. Behav.* **2016**, *11*, e1256530. [CrossRef] [PubMed]
44. Ding, C.H.; Chachin, K.; Ueda, Y.; Wang, C.Y. Inhibition of loquat enzymatic browning by sulfhydryl compounds. *Food Chem.* **2002**, *76*, 213–218. [CrossRef]
45. Espley, R.V.; Leif, D.; Plunkett, B.; Mcghie, T.; Henry-Kirk, R.; Hall, M.; Johnston, J.W.; Punter, M.P.; Boldingh, H.; Nardozza, S.; et al. Red to brown: An elevated anthocyanic response in apple drives ethylene to advance maturity and fruit flesh browning. Front. *Plant Sci.* **2019**, *10*, 1248. [CrossRef] [PubMed]
46. Luna, M.C.; Tudela, J.A.; Martínez-Sánchez, A.; Allende, A.; Marín, A.; Gil, M.L. Long-term deficit and excess of irrigation influences quality and browning related enzymes and phenolic metabolism of fresh-cut iceberg lettuce (*Lactuca sativa* L.). *Postharvest Biol. Technol.* **2012**, *73*, 37–45. [CrossRef]
47. Lin, Y.F.; Lin, Y.X.; Lin, H.T.; Zhang, S.; Chen, Y.H.; Shi, J. Inhibitory effects of propyl gallate on browning and its relationship to active oxygen metabolism in pericarp of harvested longan fruit. *LWT—Food Sci. Technol.* **2015**, *60*, 1122–1128. [CrossRef]
48. Elfalleh, W.; Hannachi, H.; Tlili, N.; Yahia, Y.; Nasri, N.; Ferchichi, A. Total phenolic contents and antioxidant activities of pomegranate peel, seed, leaf and flower. *J. Med. Plants Res.* **2012**, *6*, 4724–4730. [CrossRef]
49. Pereyra, L.; Roura, S.I.; del Valle, C.E. Phenylalanine ammonia lyase activity in minimally processed Romaine lettuce. *LWT—Food Sci. Technol.* **2005**, *38*, 67–72. [CrossRef]
50. Dong, T.; Shi, J.; Jiang, C.Z.; Feng, Y.; Cao, Y.; Wang, Q. A short-term carbon dioxide treatment inhibits the browning of fresh-cut burdock. *Postharvest Biol. Technol.* **2015**, *110*, 96–102. [CrossRef]
51. Ramakrishna, A.; Ravishankar, G.A. Influence of abiotic stress signals on secondary metabolites in plants. *Plant Signal. Behav.* **2011**, *6*, 1720–1731. [CrossRef]
52. Chen, M.Y.; Lin, H.T.; Zhang, S.; Lin, Y.F.; Chen, Y.H.; Lin, Y.X. Effects of adenosine triphosphate (ATP) treatment on postharvest physiology, quality and storage behavior of longan fruit. *Food Bioprocess Technol.* **2015**, *8*, 971–982. [CrossRef]
53. Yang, S.; Su, X.; Prasad, K.N.; Yang, B.; Cheng, G.; Chen, Y.; Yang, E.; Jiang, Y. Oxidation and peroxidation of postharvest banana fruit during softening. *Pak. J. Bot.* **2008**, *40*, 2023–2029.
54. Jiang, Y.M.; Jiang, Y.L.; Qu, H.X.; Duan, X.W.; Luo, Y.B.; Jiang, W.B. Energy aspects in ripening and senescence of harvested horticultural crops. *Stewart Postharvest Rev.* **2007**, *3*, 1–5. [CrossRef]
55. McWeeny, D.J.; Knowles, M.E.; Hearne, J.F. The chemistry of non-enzymic browning in foods and its control by sulphites. *J. Sci. Food Agric.* **1974**, *25*, 735–746. [CrossRef]
56. Lievonen, S.M.; Laaksonen, T.J.; Roos, Y.H. Nonenzymatic browning in food models in the vicinity of the glass transition: Effects of fructose, glucose, and xylose as reducing sugar. *J. Agric. Food Chem.* **2002**, *50*, 7034–7041. [CrossRef]
57. Korbel, E.; Attal, E.H.; Grabulos, J.; Lluberas, E.; Durand, N.; Morel, G.; Goli, T.; Brat, P. Impact of temperature and water activity on enzymatic and nonenzymatic reactions in reconstituted dried mango model system. *Eur. Food Res. Technol.* **2013**, *237*, 39–46. [CrossRef]
58. Fukuoka, N.; Miyata, M.; Hamada, T.; Takeshita, E. Histochemical observations and gene expression changes related to internal browning in tuberous roots of sweet potato (*Ipomea batatas*). *Plant Sci.* **2018**, *274*, 476–484. [CrossRef]
59. Mellidou, I.; Buts, K.; Hatoum, D.; Ho, Q.T.; Johnston, J.W.; Watkins, C.B.; Schaffer, R.J.; Gapper, N.E.; Giovannoni, J.J.; Rudell, D.R.; et al. Transcriptomic events associated with internal browning of apple during postharvest storage. *BMC Plant Biol.* **2014**, *14*, 328. [CrossRef]